

Original Article



OPEN ACCESS

Received: Oct 1, 2018
Revised: Nov 7, 2018
Accepted: Nov 20, 2018









Correspondence to Young Noh, MD, PhD

Department of Neurology, Gachon University
Gil Medical Center, 21 Namdong-daero 774
beon-gil, Namdong-gu, Incheon 21565, Korea.
E-mail: ynoh@gachon.ac.kr

*Cindy W Yoon and Hye Jin Jeong contributed
equally to this work.

© 2018 Korean Dementia Association
This is an Open Access article distributed
under the terms of the Creative Commons
Attribution Non-Commercial License (<https://creativecommons.org/licenses/by-nc/4.0/>)
which permits unrestricted non-commercial
use, distribution, and reproduction in any
medium, provided the original work is properly
cited.

ORCID iDs

Cindy W Yoon 
<https://orcid.org/0000-0002-4697-6610>
Hye Jin Jeong 
<https://orcid.org/0000-0003-3765-8546>
Seongho Seo 
<https://orcid.org/0000-0001-7894-0535>
Sang-Yoon Lee 
<https://orcid.org/0000-0002-6029-8553>
Mee Kyung Suh 
<https://orcid.org/0000-0003-2558-8018>
Jae-Hyeok Heo 
<https://orcid.org/0000-0003-4848-0528>
Yeong-Bae Lee 
<https://orcid.org/0000-0001-5952-1423>
Kee Hyung Park 
<https://orcid.org/0000-0001-6847-6679>

<https://dnd.or.kr>

¹⁸F-THK5351 PET Imaging in Nonfluent-Agrammatic Variant Primary Progressive Aphasia

Cindy W Yoon ^{1,*}, Hye Jin Jeong ^{2,*}, Seongho Seo ³, Sang-Yoon Lee ³,
Mee Kyung Suh ⁴, Jae-Hyeok Heo ⁵, Yeong-Bae Lee ⁶, Kee Hyung Park ⁶,
Nobuyuki Okamura ⁷, Kyoung-Min Lee ⁸, Young Noh ^{6,9}

¹Department of Neurology, Inha University School of Medicine, Incheon, Korea

²Neuroscience Research Institute, Gachon University, Incheon, Korea

³Department of Neuroscience, Gachon University College of Medicine, Incheon, Korea

⁴Department of Neurology, Samsung Medical Center, Sungkyunkwan University School of Medicine, Seoul, Korea

⁵Department of Neurology, Seoul Medical Center, Seoul, Korea

⁶Department of Neurology, Gachon University Gil Medical Center, Incheon, Korea

⁷Tohoku Medical and Pharmaceutical University, Sendai, Japan

⁸Department of Neurology, Seoul National University Hospital, Seoul National University College of Medicine, Seoul, Korea

⁹Department of Health Science and Technology, GAIHST, Gachon University, Incheon, Korea

ABSTRACT

Background and Purpose: To analyze ¹⁸F-THK5351 positron emission tomography (PET) scans of patients with clinically diagnosed nonfluent/agrammatic variant primary progressive aphasia (navPPA).

Methods: Thirty-one participants, including those with Alzheimer's disease (AD, $n=13$), navPPA ($n=3$), and those with normal control (NC, $n=15$) who completed 3 Tesla magnetic resonance imaging, ¹⁸F-THK5351 PET scans, and detailed neuropsychological tests, were included. Voxel-based and region of interest (ROI)-based analyses were performed to evaluate retention of ¹⁸F-THK5351 in navPPA patients.

Results: In ROI-based analysis, patients with navPPA had higher levels of THK retention in the Broca's area, bilateral inferior frontal lobes, bilateral precentral gyri, and bilateral basal ganglia. Patients with navPPA showed higher levels of THK retention in bilateral frontal lobes (mainly left side) compared than NC in voxel-wise analysis.

Conclusions: In our study, THK retention in navPPA patients was mainly distributed at the frontal region which was well correlated with functional-radiological distribution of navPPA. Our results suggest that tau PET imaging could be a supportive tool for diagnosis of navPPA in combination with a clinical history.

Keywords: Primary Progressive Nonfluent Aphasia; tau Protein; Neurofibrillary Tangles; Positron Emission Tomography

INTRODUCTION

Primary progressive aphasia (PPA) is a clinical dementia syndrome in which language capabilities slowly and progressively become impaired.¹ Three subtypes of PPA are recognized: nonfluent/agrammatic variant primary progressive aphasia (navPPA), semantic

Nobuyuki Okamura <https://orcid.org/0000-0002-5991-7812>Kyoung-Min Lee <https://orcid.org/0000-0002-3685-7642>Young Noh <https://orcid.org/0000-0002-9633-3314>

Funding

This study was supported by a grant (H114C1135) of the Korea Healthcare Technology R&D Project through the Korea Health Industry Development Institute (KHIDI) funded by the Ministry of Health & Welfare, Republic of Korea.

Conflicts of Interest

The authors have no financial conflicts of interest.

Author Contributions

Conceptualization: Park KH, Okamura N, Lee KM, Noh Y; Data curation: Heo JH, Lee YB, Park KH, Noh Y; Formal analysis: Yoon CW, Jeong HJ, Seo S, Lee SY, Suh MK, Heo JH, Okamura N, Noh Y; Funding acquisition: Noh Y; Investigation: Yoon CW, Seo S, Lee SY, Suh MK, Lee YB, Park KH, Noh Y; Methodology: Okamura N, Lee KM, Noh Y; Resources: Noh Y; Software: Jeong HJ; Supervision: Okamura N, Noh Y; Validation: Noh Y; Visualization: Jeong HJ, Noh Y; Writing - original draft: Yoon CW; Writing - review & editing: Noh Y.

variant PPA, and logopenic variant PPA.² Underlying pathologies of PPA are heterogeneous, including tauopathy, ubiquitinopathy (TAR-DNA binding protein 43), and Alzheimer's disease (AD) pathology.³⁻⁶ The major neuropathology of sporadic navPPA is known to be tauopathy.⁷⁻⁹

Tau positron emission tomography (PET) imaging may allow better understanding of tau aggregation and deposition in various dementia syndromes including navPPA. Several radiotracers have been developed for *in vivo* visualization of tau pathology.¹⁰ ¹⁸F-THK5351, a ¹⁸F-labeled THK arylquinoline tracer, has a high binding affinity and selectivity for tau.¹¹ However, off-target binding related to monoamine oxidase-B (MAO-B) has raised concerns about the specificity of ¹⁸F-THK5351 for tau recently.^{12,13} The objective of this study was to analyze ¹⁸F-THK5351 PET scans¹⁴ of patients with clinically diagnosed navPPA.

METHODS

Participants

Thirty-one participants were recruited from a single tertiary hospital from April 2015 to April 2016. They underwent a clinical interview and standard neurologic examination as well as structural brain magnetic resonance imaging (MRI) as described below. Three patients who were clinically diagnosed with navPPA according to guidelines proposed by Gorno-Tempini et al.¹⁴ and 13 patients who were diagnosed with probable AD according to the National Institute of Neurological and Communicative Disorders and Stroke and the Alzheimer's Disease and Related Disorders Association¹⁵ criteria were included in this study. We included AD patients as a representative group to show the pattern of THK retention. None of the 3 patients diagnosed with navPPA had a family history of dementia or movement disorder. Fifteen normal control (NC) subjects with normal cognition without history of neurologic or psychiatric illness or abnormalities detected on neurologic examination were also included. All participants underwent a comprehensive neuropsychological evaluation using the Seoul Neuropsychological Screening Battery-II.¹⁶ Disease severity was assessed by the frontotemporal lobar degeneration (FTLD) modified Clinical Dementia Rating (CDR) containing 2 more domains (behavior and language) in addition to the 6 standard domains of the CDR scale.^{17,19} In the NC group, the CDR score was zero, the Mini-Mental Status Examination (MMSE) score was above 25, and the overall neuropsychological test performance was 1.5 standard deviations (SDs) above age adjusted and education adjusted norms.

We excluded patients with structural, focal lesions on brain MRI such as stroke, intracranial hemorrhages, and evidence of traumatic brain injury, hydrocephalus, white matter hyperintensities associated with radiation, multiple sclerosis, or vasculitis. Potential secondary causes of dementia were excluded through laboratory tests such as complete blood count, vitamin B12 and folate levels, thyroid function test, metabolic profile, and syphilis serology. Apolipoprotein E (APOE) genotyping was also conducted as described previously.²⁰ Our Institutional Review Board (IRB) approved the study protocol (IRB number: GDIRB2015-272). Informed consent was obtained from all participants.

Neuropsychological tests

All participants underwent neuropsychological evaluation using a battery that included assessments for the following cognitive domains: attention, language, praxis,

visuoconstructive ability, elements of Gerstmann syndrome, visual and verbal memory, and frontal/executive function. Quantifiable tests among these evaluations included digit span test (forward and backward), the Rey-Osterrieth Complex Figure Test, the Korean version of the Boston Naming Test, the Seoul Verbal Learning Test, phonemic and semantic Controlled Oral Word Association Test, and a Stroop Test (color and word reading of 112 items during a 2-minute period). MMSE, CDR, CDR Sum of Boxes, FTLD modified CDR Sum of Boxes, and Geriatric Depression Scale results were also obtained. The Korean version of the Western Aphasia Battery (K-WAB) having subscales to assess spontaneous speech, auditory verbal comprehension, repetition, naming and word finding, reading, and writing was performed in 3 subjects diagnosed with navPPA.^{21,22}

Image acquisition and preprocessing

MRI

MRI of all participants was performed with a 3.0-T MRI scanner (Siemens with a Siemens matrix coil; Verio, Orem, Utah, USA) including a 3-dimensional (3D) magnetization prepared rapid gradient echo (MPRAGE) sequence. Imaging parameters used for 3D MPRAGE were as follows: repetition time=1900 m/s, echo time=2.93 m/s, flip angle=8°, pixel bandwidth=170 Hz/pixel, total acquisition time=4 minutes 10 seconds, and the iso-voxel resolution was 1.0 mm. Other clinical MRI sequences including fluid attenuated inversion recovery sequence were also acquired.

PET

All PET scans were acquired with a Siemens Biograph 6 Truepoint PET/computed tomography (CT) scanner (Siemens, Knoxville, TN, USA) with a list mode emission acquisition. Participants underwent a 20-minute emission scan at 90 minutes after intravenous injection of 185 MBq of ¹⁸F-flutemetamol (FLUTE). Within 3 months of undergoing the initial FLUTE PET scan, all participants underwent a 20-minute emission scan starting 50 minutes after intravenous injection of 185 MBq of THK. THK was synthesized and radiolabeled at Gachon University Neuroscience Research Institute. A low-dose CT was performed for attenuation correction prior to all scans. Images were reconstructed in a 256×256×109 matrix with a voxel size of 1.33×1.33×1.5 mm using a 2D Ordered Subset Expectation Maximization algorithm (8 iterations and 16 subsets). They were corrected for physical effects including radiation attenuation and scatter.

Image processing and analysis

THK retention was expressed as a standardized uptake value ratio (SUVR) using cerebellar gray matter as reference region. FLUTE retention was also expressed as SUVR using pons as the reference region.²³ For both regional and voxel-wise group analyses of THK retention, individual sets of PET and MRI images were processed using PMOD 3.7 (PMOD Technologies Ltd., Zurich, Switzerland) as follows. Individual PET data were co-registered to 3D MRI images and corrected for grey matter atrophy and white matter spillover using MR-based partial volume correction (PVC). For the correction, we applied the geometric transfer matrix (GTM) method^{24,25} to region of interest (ROI) data and the Müller-Gärtner (MG) method²⁶ to voxel data. These were implemented in PMOD 3.7. ROI and tissue segments with GTM and MG, respectively, were obtained from individual MR images during the PMOD-based image processing step. In PVC-corrected images, voxels with low gray-matter probability ($p < 0.2$) were masked out to prevent noise amplification. Individual 3D MRI slices were then normalized to the Montreal Neurological Institute template. Their transformation matrix was applied to MRI co-registered PVC PET images.

A voxel-wise analysis was also performed to compare regional pattern of THK retention using SPM12 (Statistical Parametric Mapping; Wellcome Trust Centre for Neuroimaging, London, UK). Before comparison, normalized PVC SUVR images were smoothed with an 8 mm Gaussian kernel to account for individual anatomical differences and improve signal to noise ratio.

To compare THK retention in each group quantitatively, we defined 14 ROIs, including the precentral cortex, inferior frontal cortex (triangular part of inferior frontal gyrus, opercular part of inferior frontal gyrus, and orbital part of left inferior frontal gyrus), Broca's area (triangular part of inferior frontal gyrus and opercular part of inferior frontal gyrus), lateral temporal cortex (superior, middle, and inferior temporal cortex), mesial temporal cortex (hippocampus, parahippocampal gyrus, and amygdala), fusiform gyrus, superior parietal cortex, inferior parietal cortex (inferior parietal, supramarginal gyrus, and angular gyrus), insula cortex, anterior and posterior cingulate gyrus (posterior cingulate gyrus and precuneus), occipital cortex (superior, middle, inferior occipital gyrus, calcarine sulcus, and cuneus), basal ganglia (putamen, caudate nucleus, and pallidum), and brainstem. By using mean and SD of regional SUVR values of 15 NCs, regional Z-scores of SUVR values were calculated.

RESULTS

Demographic and clinical characteristics

Characteristics of navPPA patients are shown in **Table 1**. Those of NC and AD groups are presented in **Supplementary Table 1**. The first navPPA case was an 82-year-old man with 16 years of education. He presented with 3-year history of slow effortful speech. He showed slow speech and used short sentences. Neuropsychiatric evaluation revealed dysfunctions in verbal memory, phonemic/semantic fluency, and frontal/executive domains. Results of his K-WAB were consistent with transcortical motor aphasia. He was found to have diffuse brain atrophy. However, predominant atrophy was seen on the left frontal area on brain MRI. High THK retention was also observed in the left frontal cortex (**Fig. 1**). FLUTE PET scan was negative for amyloid pathology.

The second case was a 73-year-old man with 6 years of education who complained of difficulties with speech production that started 1.5 years prior to his initial visit. Neuropsychiatric evaluation indicated dysfunctions in verbal memory, phonemic/semantic fluency, and frontal/executive domains. Results of his K-WAB were compatible with transcortical motor aphasia. FLUTE PET scan was negative for amyloid pathology. MRI

Table 1. Characteristics of patients with navPPA

Characteristics	Case 1	Case 2	Case 3
Age (yr)	82	73	76
Gender	Men	Men	Men
Education (yr)	16	6	6
APOE genotype	ε3/ε3	ε3/ε3	ε3/ε3
K-MMSE	26	26	29
CDR	0.5	0.5	0.5
Disease duration (mon)	36	19	12
K-WAB	Transcortical motor aphasia, slow speech, hypokinetic dysarthria, AOS	Transcortical motor aphasia, slow speech, hypokinetic dysarthria, AOS	Anomic aphasia, slow initiation of speech, spastic dysarthria, hypokinetic dysarthria, AOS

NavPPA: nonfluent/agrammatic variant primary progressive aphasia, APOE: apolipoprotein E, K-MMSE: Korean version of Mini-Mental State Examination, CDR: Clinical Dementia Rating, K-WAB, Korean version of the Western Aphasia Battery, AOS: apraxia of speech.

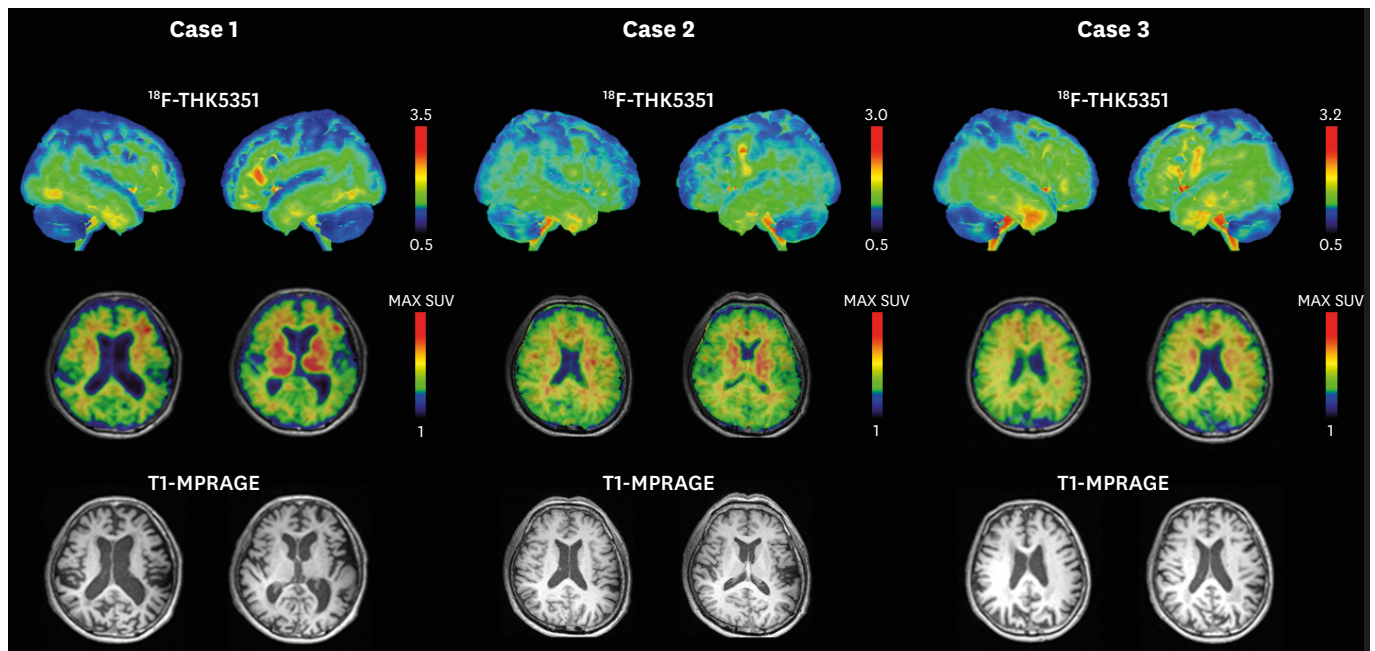


Fig. 1. ^{18}F -THK5351 PET and MRI (T1-MPRAGE) scans of navPPA patients. PET: positron emission tomography, MRI: magnetic resonance imaging, MPRAGE: magnetization prepared rapid gradient echo, navPPA: nonfluent/agrammatic variant primary progressive aphasia.

showed bilateral frontal atrophy (left > right). High THK retention was observed in the left frontal region (**Fig. 1**).

Case 3 was a 76-year-old man with 6 years of education who developed slow effortful speech from 1 year prior to enrolling in this study. Neuropsychiatric evaluation revealed dysfunction in verbal fluency. Results of his K-WAB were consistent with anomie aphasia. Atrophy on the left frontal area was seen in MRI. High THK retention was observed in the left frontal region (**Fig. 1**). FLUTE PET scan was negative for amyloid pathology.

ROI-based analysis of THK retention in navPPA, NC, and AD groups

Statistical results of ROI analysis after PVC are summarized in **Table 2**. With cut-off Z-score of 2.5, typical AD patients showed greater binding than NC in widespread cortical regions except bilateral mesial temporal, right precentral, and left anterior cingulate cortices. Patients with navPPA had higher levels of THK retention in the Broca's area, bilateral inferior frontal lobes, bilateral precentral gyri, and bilateral basal ganglia (**Table 2**). Details of ROI analysis results of 3 patients with navPPA are presented in **Supplementary Table 2**.

Voxel-based analysis of THK retention in PPA, NC, and AD groups

NavPPA vs. NC

Patients with navPPA showed higher levels of THK retention in the bilateral frontal lobe (mainly left side) than NC (**Fig. 2A**).

AD vs. NC

Patients with AD had higher levels of THK retention in widespread cortical regions (including the frontal, parietal, occipital, anterior/posterior cingulate, and mesial/lateral temporal cortices) than NC while relatively sparing the primary sensorimotor cortices bilaterally (**Fig. 2B**).

Table 2. Regional binding values of ¹⁸F-THK5351 PET in NC, AD, and navPPA patients

Regions	¹⁸ F-THK5351 SUVR					
	NC		AD		navPPA	
	Mean (SD)	Mean (SD)	Z-score	Mean (SD)	Z-score	
Precentral						
Left	0.93 (0.16)	1.37 (0.22)	2.75	2.16 (0.16)	7.69	
Right	0.84 (0.18)	1.18 (0.22)	1.89	1.33 (0.23)	2.72	
Inferior frontal						
Left	1.21 (0.22)	1.86 (0.24)	2.95	1.85 (0.36)	2.91	
Right	1.20 (0.19)	1.81 (0.32)	3.21	1.75 (0.45)	2.89	
Broca area						
Left	1.11 (0.24)	1.80 (0.24)	2.88	1.93 (0.45)	3.42	
Lateral temporal						
Left	1.42 (0.18)	2.34 (0.24)	5.11	1.80 (0.21)	2.11	
Right	1.36 (0.14)	2.36 (0.43)	5.56	1.71 (0.20)	1.94	
Mesial temporal						
Left	2.50 (0.25)	3.03 (0.68)	2.12	2.90 (0.24)	1.60	
Right	2.57 (0.23)	3.01 (0.61)	1.91	2.75 (0.24)	0.78	
Fusiform						
Left	1.62 (0.18)	2.25 (0.39)	3.59	2.02 (0.20)	2.22	
Right	1.62 (0.22)	2.28 (0.41)	3.00	2.04 (0.31)	1.91	
Superior parietal						
Left	1.16 (0.24)	2.05 (0.49)	3.71	1.64 (0.56)	2.00	
Right	1.11 (0.26)	2.21 (0.48)	4.23	1.52 (0.16)	1.58	
Inferior parietal						
Left	1.34 (0.18)	2.29 (0.39)	5.28	1.83 (0.35)	2.72	
Right	1.25 (0.14)	2.37 (0.61)	8.00	1.47 (0.90)	1.57	
Insula						
Left	1.67 (0.19)	2.42 (0.26)	3.95	2.13 (0.50)	2.42	
Right	1.71 (0.22)	2.52 (0.22)	3.68	2.23 (0.70)	2.36	
Anterior cingulate						
Left	1.93 (0.21)	2.45 (0.40)	2.48	2.36 (0.52)	2.05	
Right	1.76 (0.23)	2.35 (0.41)	2.57	2.31 (0.62)	2.39	
Posterior cingulate						
Left	1.40 (0.17)	2.27 (0.28)	5.12	1.77 (0.29)	2.18	
Right	1.33 (0.18)	2.30 (0.41)	5.39	1.55 (0.15)	1.22	
Occipital						
Left	1.18 (0.15)	1.83 (0.34)	4.33	1.46 (0.36)	1.87	
Right	1.18 (0.13)	1.90 (0.43)	5.54	1.47 (0.33)	2.23	
Basal ganglia						
Left	2.45 (0.40)	2.66 (0.33)	0.52	3.59 (0.88)	2.85	
Right	2.30 (0.36)	2.54 (0.33)	0.67	3.64 (0.47)	3.72	
Brainstem	2.17 (0.24)	2.20 (0.37)	0.13	2.68 (0.49)	2.13	

PET: positron emission tomography, NC: normal control, AD: Alzheimer's disease, navPPA: nonfluent/agrammatic variant primary progressive aphasia, SUVR: standardized uptake value ratio, SD: standard deviation.

DISCUSSION

In our study, THK retention in navPPA patients was mainly distributed at the frontal region (left > right). This regional pattern of ¹⁸F-THK5351 binding is well correlated with the functional-radiological distribution of navPPA. To account for potential confounding effects of marked cortical atrophy, all images were corrected for partial volume effects and white matter spillover in this study to confirm higher cortical THK retention.

The pathology of navPPA is heterogeneous. However, many neuropathologic studies have shown that the most common pathologic subtype of navPPA is tauopathy.^{3,7,27} Many clinically diagnosed navPPA cases are known to be often associated with corticobasal degeneration (CBD) or progressive supranuclear palsy (PSP) pathology.²⁸ Recent *in vivo* studies have

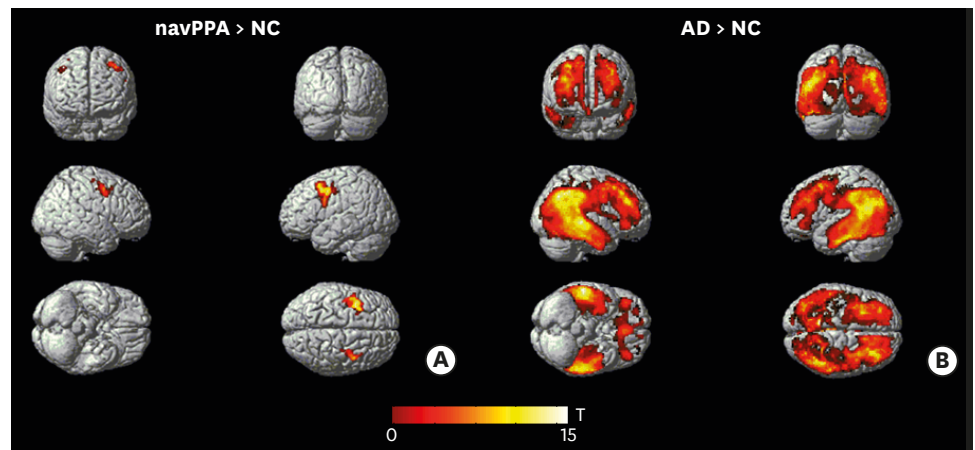


Fig. 2. Statistical parametric mapping analysis of THK SUVR images after PVC. Colored areas represent brain regions corresponding to increased THK retention from voxel-wise statistical analyses in those with navPPA (A) and AD (B) compared to NC ($p < 0.001$, uncorrected for multiple comparisons after adjusting for age, gender, and years of education, a cluster > 100).

SUVR: standardized uptake value ratio, PVC: partial volume correction, navPPA: nonfluent/agrammatic variant primary progressive aphasia, AD: Alzheimer's disease, NC: normal control, T: T value.

suggested that ^{18}F -THK5351 PET scan might be suitable for the assessment of tau deposition in 4-repeat tauopathy disease spectrum including CBD²⁹ and PSP.^{30,31} Along with these studies, our study suggests that tau PET imaging could be useful not only in AD, but also in non-AD tauopathies.

We observed that navPPA patients also showed increased THK binding in the bilateral basal ganglia. Basal ganglia atrophy and extrapyramidal sign are commonly found in navPPA patients.³²⁻³⁴ In many navPPA patients, there are clinical and pathological overlaps with CBD or PSP.²⁸ Recent reports have shown greater THK binding in the basal ganglia in PSP and CBD patients.^{29,31} However, possibility of off-target signal should also be considered because off-target signal in the MAO-B rich basal ganglia has been reported.¹²

There is a possibility that THK retention in our navPPA patients might reflect neuroinflammation or neurodegeneration rather than tau pathology itself. A recent study has shown a possibility that the interpretation of ^{18}F -THK5351 PET images could be confounded by the high MAO-B availability across the entire brain because ^{18}F -THK5351 might bind to MAO-B and tau paired helical filaments with similar affinity.¹³ MAO-B has been proposed as a biomarker for astrocytosis in various conditions associated with neuroinflammation and neurodegeneration.³⁵

Although ^{18}F -THK5351 has limited utility for selective detection of tau pathology, ^{18}F -THK5351 could be a supportive tool for diagnosis of navPPA because this tracer reflects the combination of tau pathology with associated neuroinflammatory changes and distribution is well matched with functional-radiological distribution of navPPA. An important advantage of tau PET might be its potential for early diagnosis of neurodegenerative disease due to its greater sensitivity and clarity. In some of our cases with early stage of navPPA, it was not easy to differentiate them with other types of PPA before obtaining tau PET imaging.

This study has some limitations. This was a study examining only a small number of patients. Thus, validation in a large population is needed in the future. The major caveat of our study was the lack of pathologic confirmation. Autopsy data are needed to resolve this problem.

SUPPLEMENTARY MATERIALS

Supplementary Table 1

Demographic characteristics of NC and AD groups

[Click here to view](#)

Supplementary Table 2

Regional binding values of ¹⁸F-THK5351 PET in NC, AD patients, and each navPPA patient

[Click here to view](#)

REFERENCES

1. Mesulam MM. Primary progressive aphasia--a language-based dementia. *N Engl J Med* 2003;349:1535-1542.
[PUBMED](#) | [CROSSREF](#)
2. Gorno-Tempini ML, Dronkers NF, Rankin KP, Ogar JM, Phengrasamy L, Rosen HJ, et al. Cognition and anatomy in three variants of primary progressive aphasia. *Ann Neurol* 2004;55:335-346.
[PUBMED](#) | [CROSSREF](#)
3. Josephs KA, Duffy JR, Strand EA, Whitwell JL, Layton KF, Parisi JE, et al. Clinicopathological and imaging correlates of progressive aphasia and apraxia of speech. *Brain* 2006;129:1385-1398.
[PUBMED](#) | [CROSSREF](#)
4. Hodges JR, Davies RR, Xuereb JH, Casey B, Broe M, Bak TH, et al. Clinicopathological correlates in frontotemporal dementia. *Ann Neurol* 2004;56:399-406.
[PUBMED](#) | [CROSSREF](#)
5. Kertesz A, McMonagle P, Blair M, Davidson W, Munoz DG. The evolution and pathology of frontotemporal dementia. *Brain* 2005;128:1996-2005.
[PUBMED](#) | [CROSSREF](#)
6. Forman MS, Farmer J, Johnson JK, Clark CM, Arnold SE, Coslett HB, et al. Frontotemporal dementia: clinicopathological correlations. *Ann Neurol* 2006;59:952-962.
[PUBMED](#) | [CROSSREF](#)
7. Knibb JA, Xuereb JH, Patterson K, Hodges JR. Clinical and pathological characterization of progressive aphasia. *Ann Neurol* 2006;59:156-165.
[PUBMED](#) | [CROSSREF](#)
8. Harris JM, Gall C, Thompson JC, Richardson AM, Neary D, du Plessis D, et al. Classification and pathology of primary progressive aphasia. *Neurology* 2013;81:1832-1839.
[PUBMED](#) | [CROSSREF](#)
9. Grossman M. Primary progressive aphasia: clinicopathological correlations. *Nat Rev Neurol* 2010;6:88-97.
[PUBMED](#) | [CROSSREF](#)
10. Villemagne VL, Fodero-Tavoletti MT, Masters CL, Rowe CC. Tau imaging: early progress and future directions. *Lancet Neurol* 2015;14:114-124.
[PUBMED](#) | [CROSSREF](#)
11. Harada R, Okamura N, Furumoto S, Furukawa K, Ishiki A, Tomita N, et al. ¹⁸F-THK5351: a novel PET radiotracer for imaging neurofibrillary pathology in Alzheimer disease. *J Nucl Med* 2016;57:208-214.
[PUBMED](#) | [CROSSREF](#)
12. Harada R, Ishiki A, Kai H, Sato N, Furukawa K, Furumoto S, et al. Correlations of ¹⁸F-THK5351 PET with postmortem burden of tau and astrogliosis in Alzheimer disease. *J Nucl Med* 2018;59:671-674.
[PUBMED](#) | [CROSSREF](#)
13. Ng KP, Pascoal TA, Mathotaarachchi S, Therriault J, Kang MS, Shin M, et al. Monoamine oxidase B inhibitor, selegiline, reduces ¹⁸F-THK5351 uptake in the human brain. *Alzheimers Res Ther* 2017;9:25.
[PUBMED](#) | [CROSSREF](#)
14. Gorno-Tempini ML, Hillis AE, Weintraub S, Kertesz A, Mendez M, Cappa SF, et al. Classification of primary progressive aphasia and its variants. *Neurology* 2011;76:1006-1014.
[PUBMED](#) | [CROSSREF](#)

15. McKhann G, Drachman D, Folstein M, Katzman R, Price D, Stadlan EM. Clinical diagnosis of Alzheimer's disease: report of the NINCDS-ADRDA work group under the auspices of department of health and human services task force on Alzheimer's disease. *Neurology* 1984;34:939-944.
[PUBMED](#) | [CROSSREF](#)
16. Kang Y, Jahng S, Na DL. *Seoul Neuropsychological Screening Battery*. 2nd ed. Seoul: Human Brain Research & Consulting Co., 2012.
17. Borroni B, Agosti C, Premi E, Cerini C, Cosseddu M, Paghera B, et al. The FTL D-modified Clinical Dementia Rating scale is a reliable tool for defining disease severity in frontotemporal lobar degeneration: evidence from a brain SPECT study. *Eur J Neurol* 2010;17:703-707.
[PUBMED](#) | [CROSSREF](#)
18. Kim EJ, Park KW, Lee JH, Choi S, Jeong JH, Yoon SJ, et al. Clinical and neuropsychological characteristics of a nationwide hospital-based registry of frontotemporal dementia patients in Korea: a CREDOS-FTD study. *Dement Geriatr Cogn Dis Extra* 2014;4:242-251.
[PUBMED](#) | [CROSSREF](#)
19. Knopman DS, Kramer JH, Boeve BF, Caselli RJ, Graff-Radford NR, Mendez MF, et al. Development of methodology for conducting clinical trials in frontotemporal lobar degeneration. *Brain* 2008;131:2957-2968.
[PUBMED](#) | [CROSSREF](#)
20. Lee JH, Kim SH, Kim GH, Seo SW, Park HK, Oh SJ, et al. Identification of pure subcortical vascular dementia using 11C-Pittsburgh compound B. *Neurology* 2011;77:18-25.
[PUBMED](#) | [CROSSREF](#)
21. Ahn HJ, Chin J, Park A, Lee BH, Suh MK, Seo SW, et al. Seoul neuropsychological screening battery-dementia version (SNSB-D): a useful tool for assessing and monitoring cognitive impairments in dementia patients. *J Korean Med Sci* 2010;25:1071-1076.
[PUBMED](#) | [CROSSREF](#)
22. Kim H, Na DL. Normative data on the Korean version of the Western Aphasia Battery. *J Clin Exp Neuropsychol* 2004;26:1011-1020.
[PUBMED](#) | [CROSSREF](#)
23. Thurfjell L, Lilja J, Lundqvist R, Buckley C, Smith A, Vandenberghe R, et al. Automated quantification of 18F-flutemetamol PET activity for categorizing scans as negative or positive for brain amyloid: concordance with visual image reads. *J Nucl Med* 2014;55:1623-1628.
[PUBMED](#) | [CROSSREF](#)
24. Rousset OG, Ma Y, Evans AC. Correction for partial volume effects in PET: principle and validation. *J Nucl Med* 1998;39:904-911.
[PUBMED](#)
25. Rousset OG, Collins DL, Rahmim A, Wong DF. Design and implementation of an automated partial volume correction in PET: application to dopamine receptor quantification in the normal human striatum. *J Nucl Med* 2008;49:1097-1106.
[PUBMED](#) | [CROSSREF](#)
26. Seelaar H, Kamphorst W, Rosso SM, Azmani A, Masdjedi R, de Koning I, et al. Distinct genetic forms of frontotemporal dementia. *Neurology* 2008;71:1220-1226.
[PUBMED](#) | [CROSSREF](#)
27. Mesulam M, Wicklund A, Johnson N, Rogalski E, Léger GC, Rademaker A, et al. Alzheimer and frontotemporal pathology in subsets of primary progressive aphasia. *Ann Neurol* 2008;63:709-719.
[PUBMED](#) | [CROSSREF](#)
28. Josephs KA, Petersen RC, Knopman DS, Boeve BF, Whitwell JL, Duffy JR, et al. Clinicopathologic analysis of frontotemporal and corticobasal degenerations and PSP. *Neurology* 2006;66:41-48.
[PUBMED](#) | [CROSSREF](#)
29. Kikuchi A, Okamura N, Hasegawa T, Harada R, Watanuki S, Funaki Y, et al. *In vivo* visualization of tau deposits in corticobasal syndrome by 18F-THK5351 PET. *Neurology* 2016;87:2309-2316.
[PUBMED](#) | [CROSSREF](#)
30. Vettermann F, Brendel M, Danek A, Levin J, Bartenstein P, Okamura N, et al. [18F] THK-5351 PET in patients with clinically diagnosed progressive supranuclear palsy. *J Nucl Med* 2016;57:457.
31. Ishiki A, Harada R, Okamura N, Tomita N, Rowe CC, Villemagne VL, et al. Tau imaging with [¹⁸F]THK-5351 in progressive supranuclear palsy. *Eur J Neurol* 2017;24:130-136.
[PUBMED](#) | [CROSSREF](#)
32. Gorno-Tempini ML, Ogar JM, Brambati SM, Wang P, Jeong JH, Rankin KP, et al. Anatomical correlates of early mutism in progressive nonfluent aphasia. *Neurology* 2006;67:1849-1851.
[PUBMED](#) | [CROSSREF](#)

33. Kremen SA, Mendez MF, Tsai PH, Teng E. Extrapyrarnidal signs in the primary progressive aphasias. *Am J Alzheimers Dis Other Demen* 2011;26:72-77.
[PUBMED](#) | [CROSSREF](#)
34. Ferrari J, Pontello N, Martinez-Cuitiño M, Borovinsky G, Gleichgerrcht E, Torralva T, et al. Extrapyrarnidal signs across variants of primary progressive aphasias. *Mov Disord* 2014;29 Suppl 1:598.
35. Gulyás B, Pavlova E, Kása P, Gulya K, Bakota L, Várszegi S, et al. Activated MAO-B in the brain of Alzheimer patients, demonstrated by [11C]-L-deprenyl using whole hemisphere autoradiography. *Neurochem Int* 2011;58:60-68.
[PUBMED](#) | [CROSSREF](#)